



## RESEARCH ARTICLE

# Cofluctuation analysis reveals aberrant default mode network patterns in adolescents and youths with autism spectrum disorder

Lei Li<sup>1,2,3</sup> | Xiaoran Su<sup>4,5</sup> | Qingyu Zheng<sup>2,3</sup> | Jinming Xiao<sup>2,3</sup> |  
 Xin Yue Huang<sup>2,3</sup> | Wan Chen<sup>4</sup> | Kaihua Yang<sup>4</sup> | Lei Nie<sup>4</sup> | Xin Yang<sup>4</sup> |  
 Huafu Chen<sup>1,2,3</sup>  | Shengli Shi<sup>4</sup> | Xujun Duan<sup>2,3</sup> 

<sup>1</sup>Department of Radiology, First Affiliated Hospital to Army Medical University, Chongqing, China

<sup>2</sup>The Clinical Hospital of Chengdu Brain Science Institute, MOE Key Lab for Neuroinformation, University of Electronic Science and Technology of China, Chengdu, China

<sup>3</sup>School of Life Science and Technology, Center for Information in Medicine, University of Electronic Science and Technology of China, Chengdu, China

<sup>4</sup>Medical Imaging Department, Henan Children's Hospital, Zhengzhou Children's Hospital, Children's Hospital Affiliated to Zhengzhou University, Zhengzhou, China

<sup>5</sup>Department of MR, The First Affiliated Hospital of Xinxiang Medical University, Weihui, China

## Correspondence

Xujun Duan, The Clinical Hospital of Chengdu Brain Science Institute, MOE Key Lab for Neuroinformation, University of Electronic Science and Technology of China, Chengdu 611731, China.

Email: [duanxujun@uestc.edu.cn](mailto:duanxujun@uestc.edu.cn)

Shengli Shi, Medical Imaging Department, Children's Hospital Affiliated to Zhengzhou University, Henan Children's Hospital, Zhengzhou Children's Hospital, Zhengzhou 450000, China.

Email: [s0220ssl@hotmail.com](mailto:s0220ssl@hotmail.com)

Huafu Chen, Department of Radiology, First Affiliated Hospital to Army Medical University, Chongqing 400038, China.

Email: [chenhf@uestc.edu.cn](mailto:chenhf@uestc.edu.cn)

## Funding information

Innovation Team and Talents Cultivation Program of National Administration of Traditional Chinese Medicine, Grant/Award Number: ZYYCXTD-D-202003; Fundamental Research Funds for Central Universities, Grant/Award Number: ZYGX2019Z017; National Social Science Foundation of China, Grant/Award Number: 20&ZD296; National Natural Science Foundation of China, Grant/Award Numbers: 62036003, 81871432,

## Abstract

Resting-state functional connectivity (rsFC) approaches provide informative estimates of the functional architecture of the brain, and recently-proposed cofluctuation analysis temporally unwraps FC at every moment in time, providing refined information for quantifying brain dynamics. As a brain network disorder, autism spectrum disorder (ASD) was characterized by substantial alteration in FC, but the contribution of moment-to-moment-activity cofluctuations to the overall dysfunctional connectivity pattern in ASD remains poorly understood. Here, we used the cofluctuation approach to explore the underlying dynamic properties of FC in ASD, using a large multisite resting-state functional magnetic resonance imaging (rs-fMRI) dataset (ASD = 354, typically developing controls [TD] = 446). Our results verified that the networks estimated using high-amplitude frames were highly correlated with the traditional rsFC. Moreover, these frames showed higher average amplitudes in participants with ASD than those in the TD group. Principal component analysis was performed on the activity patterns in these frames and aggregated over all subjects. The first principal component (PC1) corresponds to the default mode network (DMN), and the PC1 coefficients were greater in participants with ASD than those in the TD group. Additionally, increased ASD symptom severity was associated with the increased coefficients, which may result in excessive internally oriented cognition and social cognition deficits in individuals with ASD. Our finding highlights the utility of

Lei Li and Xiaoran Su contributed equally to this work.

This is an open access article under the terms of the [Creative Commons Attribution-NonCommercial-NoDerivs](https://creativecommons.org/licenses/by-nc-nd/4.0/) License, which permits use and distribution in any medium, provided the original work is properly cited, the use is non-commercial and no modifications or adaptations are made.

© 2022 The Authors. *Human Brain Mapping* published by Wiley Periodicals LLC.

82121003

cofluctuation approaches in prevalent neurodevelopmental disorders and verifies that the aberrant contribution of DMN to rsFC may underline the symptomatology in adolescents and youths with ASD.

## 1 | INTRODUCTION

Autism spectrum disorders (ASDs) refer to neurodevelopmental disorders characterized by impairments in social communication and interaction and stereotyped behavior and interests (American Psychiatric Association, 2013). Although these disorders have common central features, including poor social reciprocity, lack of emotional interaction, and inability to develop relationships, their broad range and individual variability contribute to the challenges in ASDs diagnosis and treatments (Elsabbagh & Johnson, 2016; Hobson & Meyer, 2005).

Previous neuroimaging studies identified functional connectivity (FC) for assessing the temporal correlation among brain areas (Rogers et al., 2007). Previous studies reported that ASD was associated with altered FC patterns in a pair of cortical midline brain regions, namely, the posterior cingulate cortex (PCC) and ventromedial prefrontal cortices, which constituted the hubs of the default mode network (DMN) (Assaf et al., 2010; Sutterer & Tranel, 2017). This network involved internally directed attention, self-referential thought, and social cognition (Uddin et al., 2007). Many studies showed that the self-reflective and social cognition deficits observed in ASD were associated with the alterations in FC within DMN nodes and from the DMN nodes to the entire brain (Washington et al., 2014; Yerys et al., 2015). Increased within network connectivity between core DMN nodes was reported in children with ASD (Lynch et al., 2013; Uddin et al., 2013). Moreover, some study found that participants with ASD exhibited over-connectivity between the medial and anterolateral temporal cortex and an aberrantly weak connectivity of the precuneus with visual cortex and basal ganglia (Lynch et al., 2013). This study also reported a significant correlation between aberrant connectivity patterns and the severity of social impairment.

Existing FC methods typically assume that time series maintain their characteristics over time. Therefore, they are usually estimated over the course of an entire scan session (Rogers et al., 2007). Recent evidence emphasized the importance of dynamic functional interactions, in which sliding window techniques were used to track fluctuations in FC across time. An arbitrary fixed window length was determined prior to analyses, and FC matrices were subsequently calculated for observations within that window. The window slides along the timeseries, and states are clustered on the basis of the dynamic FC matrices of each window (Allen et al., 2014). One study found hypervariability in ASD across numerous brain regions, thereby suggesting the presence of atypical network connectivity in multiple transient states while falling short of statistical significance in static analysis (Mash et al., 2019). Other studies demonstrated dynamic characteristic as a function of ASD symptoms. Global alterations in dynamic FC density (FCD) variabilities and atypical dynamics of intra-

and interhemispheric FCD variabilities were found in ASD (Guo et al., 2020). The within-network variance of DMN was significantly associated with the symptom severity of ASD. Besides, the atypical dynamic FC variance between DMN and sensorimotor cortex was associated with social deficits in ASD (He et al., 2018). In addition, the increased variance of widespread long-range dynamic functional connections was found in ASD, thereby suggesting that greater dynamic variance was a potential biomarker of ASD (Chen et al., 2017). Additionally, abnormal quantification of metrics of sliding window analysis, including dwell time (Yao et al., 2016) and transitions between brain states (De Lacy et al., 2017; Watanabe & Rees, 2017), was found in participants with ASD, hence supporting the evidence that ASD was characterized by transient states. Although early studies on dynamic FC and the symptom severity in ASD produced some results, the windowing procedure induced a blurring effect, thus making the localization of the time-varying connectivity in time and the assessment of the contributions made by each single frame impossible (Hindriks et al., 2016). Some emerging methods, such as coactivation patterns (CAPs), allow brain dynamics to be characterized at each single time point (Liu & Duyn, 2013). However, these approaches generally require the specification of a seed region or a threshold to determine high-activation frames. Thus, explaining precisely how these coactivity patterns are combined to give rise to the entire FC is elusive (Preti et al., 2017).

Recently, a comprehensive and mathematical method was proposed for the exact decomposition of FC into its frame-wise contributions, explicitly linking instantaneous patterns of cofluctuations to FC over long timescales (Esfahlani et al., 2020). They also found that FC and its system-level organization were driven by cofluctuations during high-amplitude frames, which were underpinned by the activation of the default mode and control networks. Meanwhile, 10 adults' data from the Midnight Scan Club (MSC, 10 resting state scans per subjects[Gordon et al., 2016]) were used to measure differential identifiability, which indicated how much more similar FC patterns were to intra-subject than to inter-subject. The results indicated that the cofluctuations of high-amplitude frames carried reliably individualized and distinguishable information. Despite this methodological innovation, latest studies produced interesting results. A recent study used two independent sampling datasets (i.e., MSC and MyConnectome [Laumann et al., 2015], a project in which a single individual was scanned >100 times) to demonstrate that the FC of a few high-amplitude frames recapitulated time-averaged FC accurately. They also extended the prior study by classifying a small subset of high-amplitude frames as "event" (Betzel et al., 2022b). The use of cofluctuation analysis showed that functional dynamic in high-amplitude frames were partly shaped by the modular organization of structural connectivity (Pope et al., 2021).

	ASD (n = 354)	TD (n = 446)	t/ $\chi^2$	p value
Age (years)	13.47 ± 3.62	13.40 ± 3.26	$t_{(798)} = 0.29$	.76 <sup>a</sup>
Sex (male/female)	301/53	382/64	$\chi^2 = 0.053$	.82 <sup>b</sup>
Handedness (right/left/mixed)	291/34/29	387/29/30	$\chi^2 = 1.25$	.54 <sup>b</sup>
FIQ	105.55 ± 17.07	112.97 ± 17.07	$t_{(798)} = -7.00$	<.05 <sup>a</sup>
Mean FD (mm)	0.15 ± 0.05	0.63 ± 0.05	$t_{(798)} = -1.26$	.21 <sup>a</sup>
ADI_R (N = 257)				
Social	19.68 ± 5.29			
Verbal	15.41 ± 4.62			
RRB	5.80 ± 3.30			
Onset	3.03 ± 2.51			
ADOS gotham				
RRB (N = 204)	2.03 ± 1.61			
Social (N = 227)	8.03 ± 2.83			
Communication (N = 227)	3.50 ± 1.64			
Total (N = 238)	11.57 ± 4.03			

**TABLE 1** Demographics and clinical characteristics of the participants

Abbreviations: ADI\_R Autism Diagnostic Interview-Revised; ADOS, the Autism Diagnostic Observation Schedule; ASD, autism spectrum disorder; FD, frame-wise displacement; FIQ, the full-scale intelligence quotient; RRB, restricted and repetitive behaviors; TD, typically developing controls.

N number of subjects.

<sup>a</sup>The p value was obtained by two sample t-test, two tailed;

<sup>b</sup>The p value was obtained by  $\chi^2$  test.

Taken together, previous studies provided evidence of the abnormal FC of the DMN in ASD, but focused mostly on the entire scan session. The contribution of moment-to-moment-activity cofluctuations to the overall dysfunctional connectivity pattern in ASD remains poorly understood. Notably, adolescence or youth (ages 8–24) is a particularly critical window for social development, thus it is an important time to investigate the neurobiological mechanism implicated in social behaviors. The current study applied the cofluctuation analysis to rs-fMRI in a large multisite sample of adolescents and youths from the ABIDE repository (ASD = 354, typically developing controls [TD] = 446). We speculate that adolescents and youths with ASD would show abnormal cofluctuations in a few frames, and such abnormalities may underline their social deficits.

## 2 | MATERIALS AND METHODS

### 2.1 | Participants

Original rs-fMRI data and phenotypes were downloaded from the ABIDE repository (ABIDEs I and II, [http://fcon\\_1000.projects.nitrc.org/indi/abide/](http://fcon_1000.projects.nitrc.org/indi/abide/)) (Di Martino et al., 2014; Martino et al., 2017). The inclusion criteria were detailed as follows: 1) subjects between 8 and 22 years of age; 2) participants with complete cortical coverage and available full IQ (FIQ), handedness, and eye state during scanning scores; 3) subjects with low levels of head motion during scanning (i.e., maximum motion <2 mm translation and 2° rotation and less than 30% frames with high frame-wise displacement [FD], as illustrated in

preprocessing); 4) full anatomical and high-quality brain images determined by manual checking; 5) well-matched dataset between the ASD and TD groups for each site generated using a data-driven algorithm that maximizes the p values of group difference in terms of age, handedness, FIQ, eye status, and mean FD; and 6) sites with more than ten subjects per group left after the aforementioned selection procedure. Finally, a well-matched dataset of 800 subjects (ASD = 354, TD = 446) from 16 sites was constructed. The demographic data is shown in Table 1.

### 2.2 | Data preprocessing

The rs-fMRI data were preprocessed using the advanced edition of the data-processing assistant for rs-fMRI (DPARSFA v4.1, <http://rfmri.org/DPARSA>) toolbox in MATLAB (Yan & Zang, 2010). The first ten images of each subject were removed to ensure a steady-state longitudinal magnetization. Slice-timing correction and realignment were applied on the remaining functional images to correct the temporal differences and head motion. The corrected data were spatially normalized to the Montreal Neurological Institute stereotaxic space by using 12-parameter affine linear transformation and nonlinear deformation and resampled to  $3 \times 3 \times 3$  mm<sup>3</sup>. This process enabled us to directly compare responses among adolescents, youths, and young adults. Previous studies suggested that anatomical differences among children as young as seven were small relative to the resolution of fMRI data, which supported the usage of a common space in a group with a broad age range (Bedny et al., 2015; Burgund

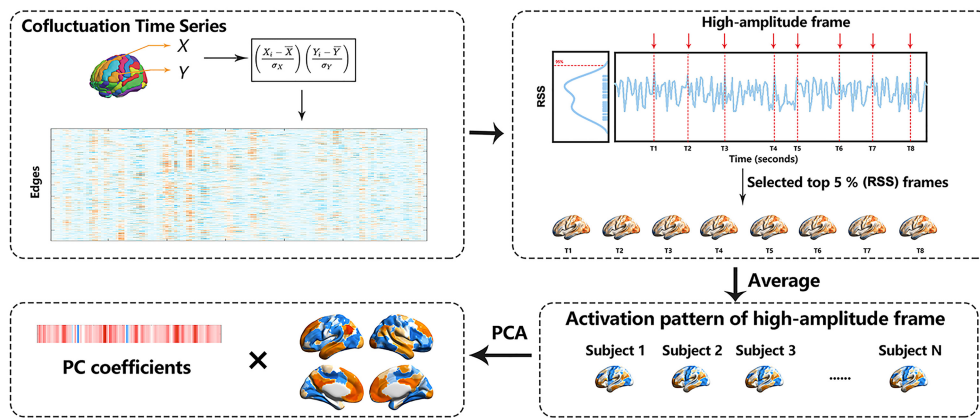


**FIGURE 1** Overview of analysis pipeline. We temporal unwrapped the Pearson correlation to generate the co-fluctuation time series for every pair of brain regions (edges). Then, we identified these moments by calculating the RSS across all the co-fluctuation time series and plotting this value as a function of time. As shown in the distribution of edge co-fluctuation amplitude, we extracted the top 5% of all time points (ordered by co-fluctuation amplitude) and obtained the average of the activity patterns of these time points within subjects. Last, we performed principal components analysis on the activity patterns in the high-amplitude frames

et al., 2002). Subsequently, all the normalized functional images were smoothed using a 6-mm full-width at half-maximum Gaussian kernel and then detrended. Next, the linear trends were removed. Signals from white matter and cerebrospinal fluid and 24 rigid body motion parameters were regressed out of the data. Subsequently, a bandpass filter (0.01–0.1 Hz) was applied on the regressed time series. Finally, given that FC was sensitive to the confounding factor of head motion, scrubbing was performed for motion correction to reduce the negative influence. When the FD exceeded 0.5 mm, the value of the signal at that point was removed. Growing evidence showed that the global signal, especially in studies of ASD (Gotts et al., 2013), may also contain valuable information (Fox et al., 2009; Schölvinck et al., 2010). Therefore, the global signal regression (GSR) was not applied.

### 2.3 | Regions-of-interest parcellation

In the current study, Schaefer et al.'s parcellation (Schaefer et al., 2018) scheme (resampled to MNI152Nlin2009cAsym standard space) was used with 200 parcels, each of which was associated with one of brain network from Yeo et al.'s seven-network parcellation (Yeo et al., 2011), namely, the visual, somatomotor, dorsal attention, ventral attention, limbic, frontoparietal task control, and DMNs.

### 2.4 | Cofluctuation time series

The strength of the FC between two brain regions was quantified as the Pearson correlation of their fMRI blood oxygen level-dependent (BOLD) time series, which was calculated as the mean value of their element-wise z-scores. The averaging step was omitted in the cofluctuation analysis. Let  $x_i = [x_i(1), \dots, x_i(T)]$  and  $x_j = [x_j(1), \dots, x_j(T)]$  be the time series recorded from voxels or parcels  $i$  and  $j$ , respectively. Similar to the Pearson correlation, we first obtained the z-score of each time series,

$Z_i = \frac{x_i - \mu_i}{\sigma_i}$ , where  $\mu_i = \frac{1}{T} \sum_t x_i(t)$  and  $\sigma_i = \frac{1}{T-1} \sum_t [x_i(t) - \mu_i]$  were the time averaged mean and SD, respectively. Subsequently, the cofluctuation of  $i$  with  $j$  was calculated as  $[Z_i \times Z_j]$ . This procedure was repeated for all pairs of parcels, thereby resulting in a set of cofluctuation (edge) time series. With  $N$  parcels, this set had  $\frac{N(N-1)}{2}$  pairs, each of length  $T$ . These elements represented the cofluctuation magnitude among the regions resolved at each moment in time.

A cofluctuation time series contains moments in time when many edges cofluctuate collectively. We identified these moments by calculating the amplitude (quantified by computing the root sum square [RSS]) across all cofluctuation time series and plotting this value as a function of time (Figure 1). We extracted the top 5% high-amplitude frames of all the time points (ordered by cofluctuation amplitude) and estimated the FC from those points alone. Then, we calculated the average RSS and activity patterns in the high-amplitude frames for each participant. In addition, the variances in the activity pattern of the high-amplitude frames in each group were obtained to characterize the fluctuation of these frames.

To understand what drove the high-amplitude frames better, we performed principal component analysis (PCA) on the activity patterns in the high-amplitude frames, which aggregated over all the subjects and scans. Then, the statistical significance of the regional PC scores was assessed nonparametrically by using permutation tests (Linting et al., 2011). The original data was permuted to obtain the permuted data set. The total number of possible permuted data set was  $n!^{m-1}$ , where  $n$  was the number of participants, and  $m$  was the number of the regional PC scores.

### 2.5 | Statistical analysis

For the demographic data, the two-sample  $t$  test was used to evaluate the differences in age, FIQ, and mean FD. The  $\chi^2$  test was performed on the handedness and the eye state.

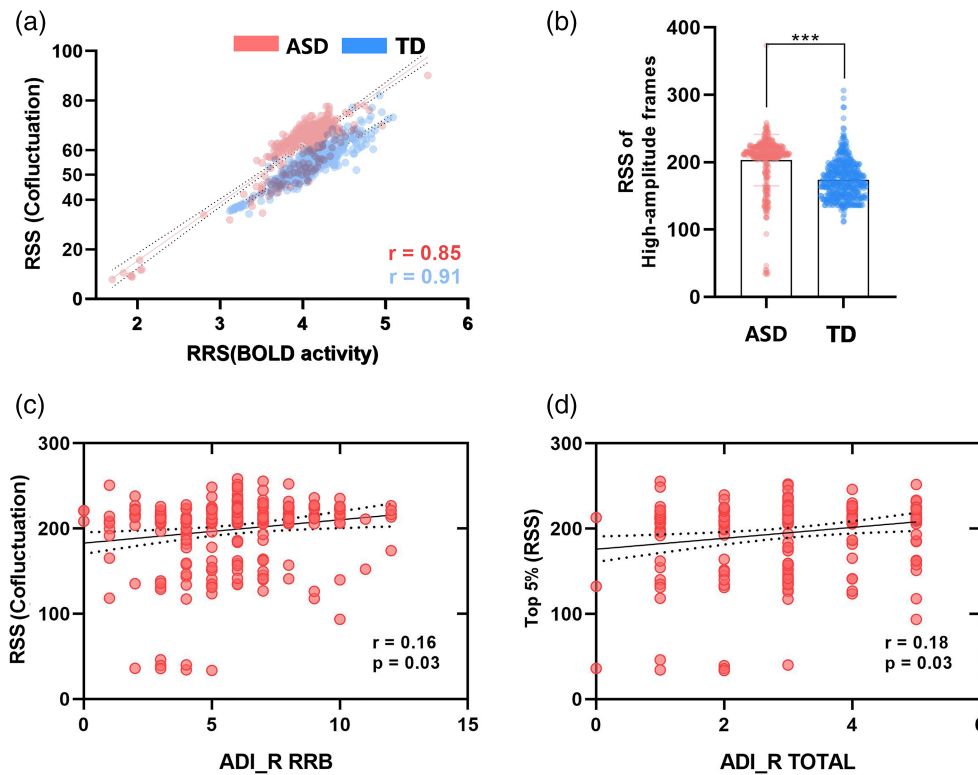


**FIGURE 2** Characteristics of co-fluctuation in high-amplitude frames. (a) Relationship of co-fluctuations with BOLD fluctuations. Pooling data from across subjects, co-fluctuation was highly related to the BOLD activity. (b) Between-group difference (ASD vs. TD) in RSS of high-amplitude frames (top 5%). \*\*\* $p < 0.0001$  (c) RSS of high-amplitude frames was significantly positive related to the RRB score in ADI\_R (FDR corrected,  $p < 0.05$ ). (d) RSS of high-amplitude frames was significantly positive related to the total score in ADI\_R (FDR corrected,  $p < 0.05$ ). ADI\_R autism diagnostic interview-revised; RRB, restricted and repetitive behaviors

In the current study, ComBat (Johnson et al., 2007) was used to reduce potential biases and non-biological variability induced by site and scanner effects. Notably, in the ComBat model, age, sex, handedness, mean FD, FIQ, and group as covariates were included to preserve important biological trends in the data and avoid overcorrection. ComBat harmonization analysis was performed using a publicly available MATLAB package hosted at <https://github.com/Jfortin1/ComBatHarmonization> (Yu et al., 2018). Next, the two-sample  $t$  test was conducted to assess the between-group differences (ASD vs. TD) in the RSS of the high-amplitude frames and the PCA coefficients. Additionally, two-way ANOVA was performed for PC1 coefficients using diagnosis (two levels: ASD and TD) and age (three levels: <12 years, 12–18 years and > 18 years) as between-subject factors. The gender, FIQ, handedness, and mean FD were taken as covariates in the model.

Given that the normality of data was vague, Spearman's correlation analysis was performed between the coefficient and social behavior scores for the ASD group. The significant threshold for multiple comparisons was set as FDR-corrected  $p < .05$ .

## 2.6 | Reproducibility analysis

Given that several critical strategies and parameter selections might influence the findings, the reproducibility of our findings, including global signal regression and the percentage of selected top high-amplitude frames, was further validated. In addition, we performed within-Group PCA in each group.

## 3 | RESULTS

### 3.1 | Group differences in high-amplitude cofluctuation events

As a first point of results, we wanted to verify whether this mathematical approach enabled us to compare the cofluctuations of network organization with the fluctuations in the BOLD time series directly. Therefore, we calculated the RSS of the cofluctuation and z-scored fMRI BOLD time series. We found that across subjects, these time series were highly correlated in the ASD ( $r = 0.85$ ) and TD groups ( $r = 0.91$ ), indicating that high-amplitude frames had a nearly one-to-one correspondence with the high-amplitude BOLD fluctuations (Figure 2a). We found that the RSS of these high-amplitude frames was significantly higher (two-sample  $t$ -test,  $p < .0001$ ; Figure 2b) in participants with ASD than those in the TD group. Additionally, we found a significant correlation (Figure 2c,d) between the RSS of high-amplitude frames and the restricted repetitive behaviors (RRB) ( $r = 0.16$ ,  $p = .03$ ) and the total score ( $r = 0.18$ ,  $p = .03$ ) in ADI-R (FDR-corrected).

### 3.2 | Abnormal DMN patterns underlie the symptom severity in participants with ASD

We estimated the rsFC by only using the fMRI BOLD data for high-amplitude time points. Next, we calculated the similarity of the rsFC estimated during high-amplitude episodes with respect to the time-

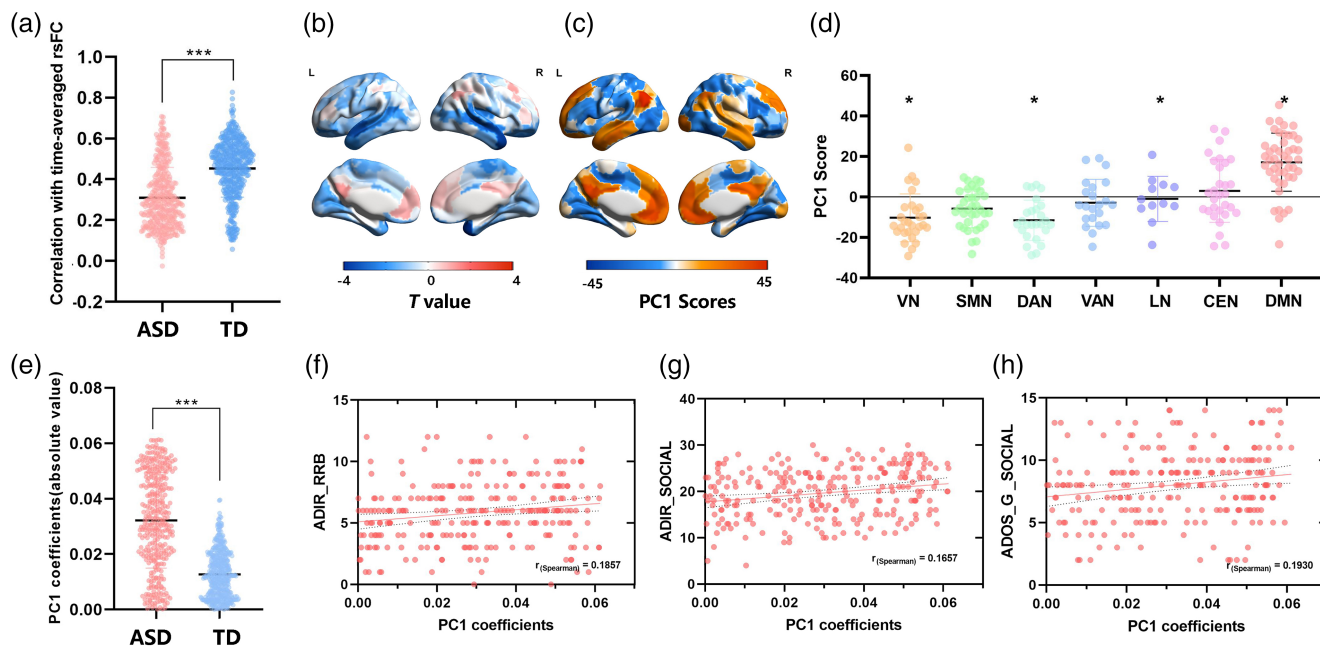


**FIGURE 3** Cofluctuation time series reveal bursty structure of resting-state FC. (a) we calculated the Pearson correlation between rsFC estimated during high-amplitude episodes with respect to time-averaged rsFC estimated using the full time series. The functional networks estimated using the top 5% of time point much more similar to traditional FC in participants with ASD than in TD group. (b) Between-group difference (ASD-TD) of variance in the activity pattern of the high-amplitude frames. (c-d) First principal component (PC1) score corresponds to the activity patterns that emphasized correlated fluctuations of default mode network. Asterisks indicate systems whose mean PC1 score was significantly greater (more positive or negative) than expected by chance (permutation test; FDR fixed at 5%) (e) value of coefficients for the PC1 were greater in the participants with ASD than TD group. (f-h) Correlation between the PC1 coefficients and clinical data in ASD. All the  $p$  values were FDR adjusted. ADI\_R autism diagnostic interview-revised; ADOS, the autism diagnostic observation schedule; RRB, restricted and repetitive behaviors

averaged rsFC estimated using the full time series. Findings showed that the high-amplitude networks were highly correlated with the rsFC, and this correlation was significantly lower in participants with ASD ( $r = 0.31 \pm 0.15$ ) than those in TD group ( $r = 0.46 \pm 0.14$ , two-sample  $t$ -test,  $p < .0001$ ; Figure 3a). Additionally, the between-group difference of variance in the activity pattern of the high-amplitude frames was determined by using two-sample  $t$ -test. In comparison with TD, the variance of the temporal cortex that belonged to the DMN was decreased in ASD (FDR,  $p < .05$ , Figure 3b).

To better understand whether high-amplitude frames were underpinned by a specific brain activity pattern, we performed PCA on the activity patterns in high-amplitude frames in the ASD and TD groups. We focused on the first principal component (PC1), which explained 32% of the total variance. Then, we mapped the component scores for PC1 onto the cortical surface and found that PC1 corresponded to a mode of activity that emphasized correlated fluctuation of the DMN and anticorrelated fluctuations of the dorsal attention and visual network (Figures 3c,d). The significances of regional PC1 scores were obtained by permutation test (FDR-corrected,  $p < .05$ ). The PC1 coefficients were much higher in participants with ASD than those in TD group (two-sample  $t$ -test,  $p < .0001$ ; Figure 3e), indicating that the DMN was descriptive of primary activity patterns in participants with ASD but less in the TD group. Additionally, the abnormal coefficients were significantly associated with the social (Figure 3f)

( $r = 0.1857$ ,  $p = .0241$ ) and RRB scores (Figure 3g) ( $r = 0.1857$ ,  $p = .0158$ ) in ADI-R and social scores ( $r = 0.1930$ ,  $p = .0158$ ) in ADOS-G (Figure 3h). FDR-correction was used for multiple comparisons. The ANOVA results of PC1 coefficients exhibited significant diagnosis-related effects. However, no significant age-specific and diagnosis-by-age interaction effect was found in the coefficients (Table 2).

In addition, as shown in Figure S1, except for PC1, other components of the PCA were not related to the DMN. Notably, we found that the second principal component (PC2) corresponded to the limbic network (Figure S1a,b), whereas the third principal component (PC3) corresponded to a mode of activity that delineated regions in ventral attention and somatomotor network (Figure S1c,d).

### 3.3 | Reproducibility results

To evaluate the stability and reproducibility of results, we repeated the main analysis by adopting different strategies and parameter selections. As a first point of validation, we calculated the results in the data with GSR. We verified that the PC1 with GSR was similar to the results without GSR (Figure S2). We re-analyzed the selection of the different percentages of top high-amplitude frames by using a broad range of threshold (0%–60%) to estimate whether it affected

	Sum of squares	Mean squares (MS)	F	p value
Main effect of age	0.002	0.001	3.068	.061
Main effect of diagnosis	0.027	0.027	164.818	.000
Diagnosis-by-age interaction effect	0.000	0.000	2.930	.087

**TABLE 2** Analysis of variance (ANOVA) results of PC1 coefficient

the results. We found that the correlation between rsFC estimated during high-amplitude frames and the time-averaged rsFC was greater in ASD than in the TD group over a range of thresholds (Figure S3a). We also found that the RSS of high-amplitude frames was greater in ASD (Figure S3b). In addition, the PC1 score patterns were robust (Figure S3c–f).

We noted that another strategy for comparing the ASD and TD was to analyze them by adopting within-Group PCA in each group. We found PC1<sub>group</sub> explained 66.6% of the total variance in the ASD group and 20.9% of that in the TD group. Although the PC1<sub>group</sub> scores of the two groups exhibited similar activities in DMN (Figure S4), we found statistically significant differences in the dorsal attention, limbic, and default mode networks (Figure S4g–h) (ASD > TD, FDR-corrected,  $p < 0.05$ ). To explore whether the lower explained variance of PC1<sub>group</sub> of TD was due to an over-decomposition of the components, we also retained the other principal components in the within-Group PCA. The first 10 components explained 84.1% of the total variance in the ASD group (Figure S4c), but only explained 63.53% of the total variance in TD (Figure S4f). Moreover, although the PC3<sub>group</sub> of the TD also emphasized the activity in the DMN, the remaining principal component in the ASD and TD groups did not exhibit this pattern (Figure S5). Viewed collectively, DMN made an overwhelming contribution to the FC in participants with ASD (PC1<sub>group</sub>) compared with the TD group (PC1<sub>group</sub> + PC3<sub>group</sub>).

## 4 | DISCUSSION

Here, we used a cofluctuation approach to temporally unwrap the Pearson correlations to examine the relationships between the functional brain dynamics and dysfunctional symptomatology in ASD. This simple procedure enables us to decompose FC into individual cofluctuation frames. The entire brain's FC and its system-level organization could be represented by a relatively small number of frames, which exhibit the strongest cofluctuation amplitude. We found that these frames showed fewer average amplitudes in participants with ASD than those in the TD group. Then, we performed PCA on the activity patterns in these high-amplitude frames, which aggregated over all subjects. We focused on the PC1 and found that it corresponded to DMN. Additionally, the abnormalities in the coefficients for PC1 were associated with the deficits of ASD. Our finding highlights the utility of cofluctuation approaches in prevalent neurodevelopmental disorders and verifies that altered DMNs may underline the social deficits in adolescents and youths with ASD.

ASD were widely considered associated with atypical patterns of functional brain connectivity in large-scale brain networks (Uddin

et al., 2013; Vissers et al., 2012). Most of these studies focused on characterizing dynamic brain patterns and utilized sliding window dynamic FC approaches that are known for potential pitfalls, such as arbitrary window sizes (Lurie et al., 2020; Preti et al., 2017). Many novel studies verified the reliability of a recently-proposed method in several independently acquired datasets, which enabled us to unwrap Pearson correlations to generate the time series of interregional cofluctuations along network edges (Betzel et al., 2022; Betzel et al., 2022b; Liu et al., 2021; Pope et al., 2021). In the current study, we leveraged this cofluctuation method to decompose FC into its frame-wise contributions in participants with ASD. In the ASD and TD groups, the RSS of the cofluctuation was highly correlated with the z-scored fMRI BOLD in the high-amplitude frames, indicating that high-amplitude frames had a nearly one-to-one correspondence with high-amplitude BOLD fluctuations. Critically, the FC of these frames was exactly equal to the whole-brain static FC, which was consistent with previous findings (Esfahlani et al., 2020). Additionally, our findings hint at a crucial link between the instantaneous fluctuations in BOLD activity and the organization of the resting state FC. We demonstrated that the DMN was primarily responsible for driving the high-amplitude frames in the ASD and TD groups. Notably, other state-based analyses of brain dynamics reported similar patterns of activity (Cornblath et al., 2020; Karapanagiotidis et al., 2020). Although this mode made the greatest contribution, other modes were also likely to make nontrivial contributions, such as the control, ventral attention, and somatomotor network modes. All these patterns may recombine in different proportions according to task complexity and domain (Yarkoni et al., 2011) across individuals (Gratton et al., 2018).

The DMN is an important network that shows a substantial overlap with the “social brain” network (Blakemore, 2008), which has been hypothesized to be a candidate locus of pathology in ASD. This network includes the medial prefrontal cortex, the posterior cingulate cortex and the adjoining precuneus, the lateral parietal regions, and the temporal regions (Fox et al., 2005; Raichle et al., 2001). Some studies proposed the involvement of the DMN in processing one's own emotional state (Buckner et al., 2008), self-referential thinking (Gusnard et al., 2001; Gusnard & Raichle, 2001), thoughts about self-versus others and theory of mind (Li et al., 2014), and autobiographical memory (Andrews-Hanna et al., 2010).

We found that DMN showed aberrant contribution to rsFC in participants with ASD, which was associated with RRB and social deficits. Previous rsFC study demonstrated that DMN was among the most disrupted functional networks in ASD (Glerean et al., 2016; Moseley et al., 2015), which was associated with social deficits in children and adults with ASD (Padmanabhan et al., 2017). Our results are consistent with the wealth of static FC research, which implicates

over-connectivity of the DMN as underlying social deficits in ASD (Anderson, 2008; Elton et al., 2016; Hogeveen et al., 2018; Redcay et al., 2013). Moreover, our results served as a compliment to static analyses by demonstrating that DMN dysfunction was not only limited to increase connectivity between nodes but also increase the contributions of momentary cofluctuations to the overall FC pattern. As mentioned earlier, in the within-Group-PCA, a particular activity pattern that involved the default regions was primarily responsible for the rsFC in the TD group. Although this mode made the greatest contribution, ventral attention and the somatomotor network also made contributions. However, the DMN made an overwhelming contribution to the FC in participants with ASD. Additionally, compared with TD, the variance of the DMN was decreased in ASD. These phenomena probably occurred because ASD decreased functional flexibility or the overly stable dynamic properties of the brain (Uddin, 2021). In the current study, the altered DMN patterns were highly correlated with the RRB in participants with ASD. The ability to flexibly switch among different patterns of thought and reference frames was a critical feature of the adaptive social function (Padmanabhan et al., 2017). Aberrancies in DMN patterns contributed to the atypical integration of information about the self in relation to “other” and impairments in the ability to attend to socially relevant stimuli flexibly (Padmanabhan et al., 2017). This finding is consistent with those of recent studies that reported on reducing transitions between the brain state configurations in ASD (Watanabe & Rees, 2017).

Although a proliferation of resting-state connectivity studies on participants with ASD has been witnessed in the past few years, the results are inconsistent. These “inconsistencies” likely reflect developmental changes, as well as individual heterogeneity in ASD (Uddin et al., 2013). Existing studies demonstrated that spontaneous brain activity is aging globally (Xing, 2021). Over typical development, intrinsic FC within DMN nodes increased between childhood and adulthood (Supekar et al., 2010). In ASD, no consistent evidence of such increases in DMN connectivity with age was found (Vissers et al., 2012; Washington et al., 2014). Some studies found mixed patterns of under- and over-connectivity in adolescents with ASD relative to the TD group (Doyle-Thomas et al., 2015; Jann et al., 2015). Therefore, in the current study, ANOVA was further performed to probe the effect of age. The results exhibited significant diagnosis-related effects. However, no significant age-specific and diagnosis-by-age interaction effect was found in the coefficients, suggesting that the atypical spontaneous brain activity of DMN in ASD was not affected by age. Even so, the mechanism underlying the shift in DMN connectivity patterns in adolescence is not fully understood in ASD yet. As such, further longitudinal exploration is necessary to understand the developmental changes and their impact on symptomatology.

#### 4.1 | Limitations

A few limitations of the current work should be noted. First, our sample includes data collected at 16 different sites. Although the sample

size and statistical power increase, the use of data across multiple sites presents its own limitations in that inter-site variability may affect the analyses. Although we used advanced multi-center correction methods (i.e., COMBAT) to reduce potential biases and non-biological variability induced by site and scanner effects, we could not be sure that inherent between-site effects were completely accounted for. Furthermore, similar to most ASD studies, our sample consisted mostly of males. Although sex was regressed in our statistical analysis, this imbalance of males to females may fail to account for differences in the brain activity of the two gender. To the best of our knowledge, ASD is a neurodevelopmental disorder. Unfortunately, ABIDE is a cross-sectional repository. Although the effects of age and interaction effect between age and group was analyzed in the current study, further studies using longitudinal data are needed to explore the developmental change in ASD. Another potential strategy, normative model, is analogous to growth charts used in pediatric medicine, mapping the height or weight as a function of age in a reference population (Cole, 2012; Marquand et al., 2019). This approach has been increasingly used to map variations between demographic, cognitive, clinical, or behavioral variables and quantitative brain readouts derived from neuroimaging (such as brain volume (Marquand et al., 2019, Wolfers et al., 2020, Ziegler et al., 2014), cortical thickness (Bethlehem et al., 2018; Zabihi et al., 2019), brain activity derived from task fMRI (Marquand et al., 2016) and rsFC (Kessler et al., 2016)), providing statistical inferences at the individual level based on the extent to which each individual deviate from the normative range. Importantly, previous multisite studies demonstrated stability and robustness of normal models across the life span (Bethlehem et al., 2022; Shan et al., 2022). However, measurement using in the current study might not be able to effectively capture the life-span developmental changes in ASD, and a potential reason might be the state-dependent nature of the moment-to moment activity cofluctuations in high-amplitude frames. Future studies are needed to examine age-dependent functional metrics for delineating the extent to which brain dynamics in ASD deviates from the normative range, from a developmental framework.

## 5 | CONCLUSION

In summary, the findings of this study were built on the growing body of literature on the use of cofluctuation approach in the investigation of neurodevelopmental disorders, particularly ASD. We used this approach to decompose the functional connections into their exact frame-wise contributions and observed the aberrant DMN pattern and overly stable dynamic properties in participants with ASD. Consistent with previous findings, our results suggested that the dysfunction in the DMN is a potential endophenotype for the behavioral deficits in ASD.

#### ACKNOWLEDGMENTS

This work was supported by the National Natural Science Foundation of China (Grant Nos. 81871432 [to XD], 82121003 [to HC],



62036003 [to HC], Fundamental Research Funds for Central Universities (Grant No.ZYGX2019Z017 [to XD]), Innovation Team and Talents Cultivation Program of National Administration of Traditional Chinese Medicine (Grant No.ZYYCXTD-D-202003 [to HC]) and National Social Science Foundation of China(Grant No. 20&ZD296 [to XD]).

## DATA AVAILABILITY STATEMENT

Original rs-fMRI data and phenotypes were downloaded from the ABIDE repository (ABIDEs I and II, [http://fcon\\_1000.projects.nitrc.org/indi/abide/](http://fcon_1000.projects.nitrc.org/indi/abide/)).

## ORCID

Huafu Chen  <https://orcid.org/0000-0002-4062-4753>

Xujun Duan  <https://orcid.org/0000-0001-8543-2117>

## REFERENCES

- Allen, E. A., Damaraju, E., Plis, S. M., Erhardt, E. B., Eichele, T., & Calhoun, V. D. (2014). Tracking whole-brain connectivity dynamics in the resting state. *Cerebral Cortex*, 24(3), 663–676.
- American Psychiatric Association. (2013). *Diagnostic and statistical manual of mental disorders (DSM-5®)*. American Psychiatric Pub.
- Anderson, G. M. (2008). The potential role for emergence in autism. *Autism Research*, 1(1), 18–30.
- Andrews-Hanna, J. R., Reidler, J. S., Huang, C., & Buckner, R. L. (2010). Evidence for the default network's role in spontaneous cognition. *Journal of Neurophysiology*, 104(1), 322–335.
- Assaf, M., Jagannathan, K., Calhoun, V. D., Miller, L., Stevens, M. C., Sahl, R., O'Boyle, J. G., Schultz, R. T., & Pearson, G. D. (2010). Abnormal functional connectivity of default mode sub-networks in autism spectrum disorder patients. *NeuroImage*, 53(1), 247–256.
- Bedny, M., Richardson, H., & Saxe, R. (2015). "Visual" cortex responds to spoken language in blind children. *Journal of Neuroscience*, 35(33), 11674–11681.
- Bethlehem, R. A., J. Seidlitz, R. Romero-Garcia and M. V. Lombardo (2018). *Using normative age modelling to isolate subsets of individuals with autism expressing highly age-atypical cortical thickness features*. bioRxiv: 252593.
- Bethlehem, R. A., Seidlitz, J., White, S. R., Vogel, J. W., Anderson, K. M., Adamson, C., Adler, S., Alexopoulos, G. S., Anagnostou, E., & Areces-Gonzalez, A. (2022). Brain charts for the human lifespan. *Nature*, 604(7906), 525–533.
- Betzell, R. F., Cutts, S. A., Greenwell, S., Faskowitz, J., & Sporns, O. (2022). Individualized event structure drives individual differences in whole-brain functional connectivity. *NeuroImage*, 252, 118993.
- Betzell, R., S. Cutts, J. Tanner, S. Greenwell, T. Varley, J. Faskowitz and O. Sporns (2022). *Hierarchical organization of spontaneous co-fluctuations in densely-sampled individuals using fMRI*. bioRxiv.
- Blakemore, S.-J. (2008). Development of the social brain during adolescence. *Quarterly Journal of Experimental Psychology*, 61(1), 40–49.
- Buckner, R. L., J. R. Andrews-Hanna and D. L. Schacter (2008). *The brain's default network: anatomy, function, and relevance to disease*.
- Burgund, E. D., Kang, H. C., Kelly, J. E., Buckner, R. L., Snyder, A. Z., Petersen, S. E., & Schlaggar, B. L. (2002). The feasibility of a common stereotactic space for children and adults in fMRI studies of development. *NeuroImage*, 17(1), 184–200.
- Chen, H., Nomi, J. S., Uddin, L. Q., Duan, X., & Chen, H. (2017). Intrinsic functional connectivity variance and state-specific under-connectivity in autism. *Human Brain Mapping*, 38(11), 5740–5755.
- Cole, T. J. (2012). The development of growth references and growth charts. *Annals of Human Biology*, 39(5), 382–394.
- Cornblath, E. J., Ashourvan, A., Kim, J. Z., Betzel, R. F., Ciric, R., Adebimpe, A., Baum, G. L., He, X., Ruparel, K., & Moore, T. M. (2020). Temporal sequences of brain activity at rest are constrained by white matter structure and modulated by cognitive demands. *Communications Biology*, 3(1), 1–12.
- De Lacy, N., Doherty, D., King, B., Rachakonda, S., & Calhoun, V. (2017). Disruption to control network function correlates with altered dynamic connectivity in the wider autism spectrum. *NeuroImage: Clinical*, 15, 513–524.
- Di Martino, A., Yan, C.-G., Li, Q., Denio, E., Castellanos, F. X., Alaerts, K., Anderson, J. S., Assaf, M., Bookheimer, S. Y., & Dapretto, M. (2014). The autism brain imaging data exchange: Towards a large-scale evaluation of the intrinsic brain architecture in autism. *Molecular Psychiatry*, 19(6), 659–667.
- Doyle-Thomas, K. A., Lee, W., Foster, N. E., Tryfon, A., Ouimet, T., Hyde, K. L., Evans, A. C., Lewis, J., Zwaigenbaum, L., & Anagnostou, E. (2015). Atypical functional brain connectivity during rest in autism spectrum disorders. *Annals of Neurology*, 77(5), 866–876.
- Elsabbagh, M., & Johnson, M. H. (2016). Autism and the social brain: The first-year puzzle. *Biological Psychiatry*, 80(2), 94–99.
- Elton, A., Di Martino, A., Hazlett, H. C., & Gao, W. (2016). Neural connectivity evidence for a categorical-dimensional hybrid model of autism spectrum disorder. *Biological Psychiatry*, 80(2), 120–128.
- Esfahlani, F. Z., Jo, Y., Faskowitz, J., Byrge, L., Kennedy, D. P., Sporns, O., & Betzel, R. F. (2020). High-amplitude co-fluctuations in cortical activity drive functional connectivity. *Proceedings of the National Academy of Sciences*, 117(45), 28393–28401.
- Fox, M. D., Snyder, A. Z., Vincent, J. L., Corbetta, M., Van Essen, D. C., & Raichle, M. E. (2005). The human brain is intrinsically organized into dynamic, anticorrelated functional networks. *Proceedings of the National Academy of Sciences*, 102(27), 9673–9678.
- Fox, M. D., Zhang, D., Snyder, A. Z., & Raichle, M. E. (2009). The global signal and observed anticorrelated resting state brain networks. *Journal of Neurophysiology*, 101(6), 3270–3283.
- Glerean, E., Pan, R. K., Salmi, J., Kujala, R., Lahnakoski, J. M., Roine, U., Nummenmaa, L., Leppämäki, S., Nieminen-von Wendt, T., & Tani, P. (2016). Reorganization of functionally connected brain subnetworks in high-functioning autism. *Human Brain Mapping*, 37(3), 1066–1079.
- Gordon, E. M., Laumann, T. O., Adeyemo, B., Huckins, J. F., Kelley, W. M., & Petersen, S. E. (2016). Generation and evaluation of a cortical area parcellation from resting-state correlations. *Cerebral Cortex*, 26(1), 288–303.
- Gotts, S. J., Saad, Z. S., Jo, H. J., Wallace, G. L., Cox, R. W., & Martin, A. (2013). The perils of global signal regression for group comparisons: A case study of autism Spectrum disorders. *Frontiers in Human Neuroscience*, 7, 356.
- Gratton, C., Laumann, T. O., Nielsen, A. N., Greene, D. J., Gordon, E. M., Gilmore, A. W., Nelson, S. M., Coalson, R. S., Snyder, A. Z., & Schlaggar, B. L. (2018). Functional brain networks are dominated by stable group and individual factors, not cognitive or daily variation. *Neuron*, 98(2), 439–452. e435.
- Guo, X., Duan, X., Chen, H., He, C., Xiao, J., Han, S., Fan, Y. S., Guo, J., & Chen, H. (2020). Altered inter- and intrahemispheric functional connectivity dynamics in autistic children. *Human Brain Mapping*, 41(2), 419–428.
- Gusnard, D. A., Akbudak, E., Shulman, G. L., & Raichle, M. E. (2001). Medial prefrontal cortex and self-referential mental activity: Relation to a default mode of brain function. *Proceedings of the National Academy of Sciences*, 98(7), 4259–4264.
- Gusnard, D. A., & Raichle, M. E. (2001). Searching for a baseline: Functional imaging and the resting human brain. *Nature Reviews Neuroscience*, 2(10), 685–694.
- He, C., Chen, Y., Jian, T., Chen, H., Guo, X., Wang, J., Wu, L., Chen, H., & Duan, X. (2018). Dynamic functional connectivity analysis reveals

- decreased variability of the default-mode network in developing autistic brain. *Autism Research*, 11(11), 1479–1493.
- Hindriks, R., Adhikari, M. H., Murayama, Y., Ganzetti, M., Mantini, D., Logothetis, N. K., & Deco, G. (2016). Can sliding-window correlations reveal dynamic functional connectivity in resting-state fMRI? *NeuroImage*, 127, 242–256.
- Hobson, R. P., & Meyer, J. A. (2005). Foundations for self and other: A study in autism. *Developmental Science*, 8(6), 481–491.
- Hogeveen, J., Krug, M. K., Elliott, M. V., & Solomon, M. (2018). Insular-retrosplenial cortex overconnectivity increases internalizing via reduced insight in autism. *Biological Psychiatry*, 84(4), 287–294.
- Jann, K., Hernandez, L. M., Beck-Pancer, D., McCarron, R., Smith, R. X., Dapretto, M., & Wang, D. J. (2015). Altered resting perfusion and functional connectivity of default mode network in youth with autism spectrum disorder. *Brain and behavior*, 5(9), e00358.
- Johnson, W. E., Li, C., & Rabinovic, A. (2007). Adjusting batch effects in microarray expression data using empirical Bayes methods. *Biostatistics*, 8(1), 118–127.
- Karapanagiotidis, T., Vidaurre, D., Quinn, A. J., Vatansever, D., Poerio, G. L., Turnbull, A., Ho, N. S. P., Leech, R., Bernhardt, B. C., & Jefferies, E. (2020). The psychological correlates of distinct neural states occurring during wakeful rest. *Scientific Reports*, 10(1), 1–11.
- Kessler, D., Angstadt, M., & Sripada, C. (2016). Growth charting of brain connectivity networks and the identification of attention impairment in youth. *JAMA Psychiatry*, 73(5), 481–489.
- Laumann, T. O., Gordon, E. M., Adeyemo, B., Snyder, A. Z., Joo, S. J., Chen, M.-Y., Gilmore, A. W., McDermott, K. B., Nelson, S. M., & Dosenbach, N. U. (2015). Functional system and areal organization of a highly sampled individual human brain. *Neuron*, 87(3), 657–670.
- Li, W., Mai, X., & Liu, C. (2014). The default mode network and social understanding of others: What do brain connectivity studies tell us. *Frontiers in Human Neuroscience*, 8, 74.
- Linting, M., Van Os, B. J., & Meulman, J. J. (2011). Statistical significance of the contribution of variables to the PCA solution: An alternative permutation strategy. *Psychometrika*, 76(3), 440–460.
- Liu, X., & Duyn, J. H. (2013). Time-varying functional network information extracted from brief instances of spontaneous brain activity. *Proceedings of the National Academy of Sciences*, 110(11), 4392–4397.
- Liu, Z.-Q., B. Vázquez-Rodríguez, R. N. Spreng, B. C. Bernhardt, R. F. Betzel and B. Misic (2021). *Time-resolved structure-function coupling in brain networks*. bioRxiv.
- Lurie, D. J., Kessler, D., Bassett, D. S., Betzel, R. F., Breakspear, M., Kheilholz, S., Kucyi, A., Liégeois, R., Lindquist, M. A., & McIntosh, A. R. (2020). Questions and controversies in the study of time-varying functional connectivity in resting fMRI. *Network Neuroscience*, 4(1), 30–69.
- Lynch, C. J., Uddin, L. Q., Supekar, K., Khouzam, A., Phillips, J., & Menon, V. (2013). Default mode network in childhood autism: Posteromedial cortex heterogeneity and relationship with social deficits. *Biological Psychiatry*, 74(3), 212–219.
- Marquand, A. F., Kia, S. M., Zabihi, M., Wolfers, T., Buitelaar, J. K., & Beckmann, C. F. (2019). Conceptualizing mental disorders as deviations from normative functioning. *Molecular Psychiatry*, 24(10), 1415–1424.
- Marquand, A. F., Rezek, I., Buitelaar, J., & Beckmann, C. F. (2016). Understanding heterogeneity in clinical cohorts using normative models: Beyond case-control studies. *Biological Psychiatry*, 80(7), 552–561.
- Martino, A. D., Oconnor, D., Chen, B., Alaerts, K., Anderson, J. S., Assaf, M., Balsters, J. H., Baxter, L. C., Beggato, A., & Bernaerts, S. (2017). Enhancing studies of the connectome in autism using the autism brain imaging data exchange II. *Scientific Data*, 4, 170010.
- Mash, L. E., Linke, A. C., Olson, L. A., Fishman, I., Liu, T. T., & Müller, R. A. (2019). Transient states of network connectivity are atypical in autism: A dynamic functional connectivity study. *Human Brain Mapping*, 40(8), 2377–2389.
- Moseley, R., Ypma, R., Holt, R., Floris, D., Chura, L., Spencer, M., Baron-Cohen, S., Suckling, J., Bullmore, E., & Rubinov, M. (2015). Whole-brain functional hypoconnectivity as an endophenotype of autism in adolescents. *NeuroImage: Clinical*, 9, 140–152.
- Padmanabhan, A., Lynch, C. J., Schaer, M., & Menon, V. (2017). The default mode network in autism. *Biological Psychiatry: Cognitive Neuroscience and Neuroimaging*, 2(6), 476–486.
- Pope, M., Fukushima, M., Betzel, R. F., & Sporns, O. (2021). Modular origins of high-amplitude co-fluctuations in fine-scale functional connectivity dynamics. *Proceedings of the National Academy of Sciences*, 118(46), e2109380118.
- Preti, M. G., Bolton, T. A., & Van De Ville, D. (2017). The dynamic functional connectome: State-of-the-art and perspectives. *NeuroImage*, 160, 41–54.
- Raichle, M. E., MacLeod, A. M., Snyder, A. Z., Powers, W. J., Gusnard, D. A., & Shulman, G. L. (2001). A default mode of brain function. *Proceedings of the National Academy of Sciences*, 98(2), 676–682.
- Redcay, E., Moran, J. M., Mavros, P. L., Tager-Flusberg, H., Gabrieli, J. D., & Whitfield-Gabrieli, S. (2013). Intrinsic functional network organization in high-functioning adolescents with autism spectrum disorder. *Frontiers in Human Neuroscience*, 7, 573.
- Rogers, B. P., Morgan, V. L., Newton, A. T., & Gore, J. C. (2007). Assessing functional connectivity in the human brain by fMRI. *Magnetic Resonance Imaging*, 25(10), 1347–1357.
- Schaefer, A., Kong, R., Gordon, E. M., Laumann, T. O., Zuo, X.-N., Holmes, A. J., Eickhoff, S. B., & Yeo, B. T. (2018). Local-global parcellation of the human cerebral cortex from intrinsic functional connectivity MRI. *Cerebral Cortex*, 28(9), 3095–3114.
- Schölvinck, M. L., Maier, A., Frank, Q. Y., Duyn, J. H., & Leopold, D. A. (2010). Neural basis of global resting-state fMRI activity. *Proceedings of the National Academy of Sciences*, 107(22), 10238–10243.
- Shan, X., Uddin, L. Q., Xiao, J., He, C., Ling, Z., Li, L., Huang, X., Chen, H., & Duan, X. (2022). Mapping the heterogeneous brain structural phenotype of autism spectrum disorder using the normative model. *Biological Psychiatry*, 91, 967–976.
- Supekar, K., Uddin, L. Q., Prater, K., Amin, H., Greicius, M. D., & Menon, V. (2010). Development of functional and structural connectivity within the default mode network in young children. *NeuroImage*, 52(1), 290–301.
- Sutterer, M. J., & Tranel, D. (2017). Neuropsychology and cognitive neuroscience in the fMRI era: A recapitulation of localizationist and connectionist views. *Neuropsychology*, 31(8), 972–980.
- Uddin, L. Q. (2021). Brain mechanisms supporting flexible cognition and behavior in adolescents with autism spectrum disorder. *Biological Psychiatry*, 89(2), 172–183.
- Uddin, L. Q., Iacoboni, M., Lange, C., & Keenan, J. P. (2007). The self and social cognition: The role of cortical midline structures and mirror neurons. *Trends in Cognitive Sciences*, 11(4), 153–157.
- Uddin, L. Q., Supekar, K., & Menon, V. (2013). Reconceptualizing functional brain connectivity in autism from a developmental perspective. *Frontiers in Human Neuroscience*, 7, 458.
- Visser, M. E., Cohen, M. X., & Geurts, H. M. (2012). Brain connectivity and high functioning autism: A promising path of research that needs refined models, methodological convergence, and stronger behavioral links. *Neuroscience & Biobehavioral Reviews*, 36(1), 604–625.
- Washington, S. D., Gordon, E. M., Brar, J., Warburton, S., Sawyer, A. T., Wolfe, A., Mease-Ference, E. R., Girton, L., Hailu, A., & Mbwana, J. (2014). Dysmaturational of the default mode network in autism. *Human Brain Mapping*, 35(4), 1284–1296.
- Watanabe, T., & Rees, G. (2017). Brain network dynamics in high-functioning individuals with autism. *Nature Communications*, 8(1), 1–14.
- Wolfers, T., Beckmann, C. F., Hoogman, M., Buitelaar, J. K., Franke, B., & Marquand, A. F. (2020). Individual differences v. the average patient:

- Mapping the heterogeneity in ADHD using normative models. *Psychological Medicine*, 50(2), 314–323.
- Xing, X.-X. (2021). Globally aging cortical spontaneous activity revealed by multiple metrics and frequency bands using resting-state functional MRI. *Frontiers in Aging Neuroscience*, 13, 803436.
- Yan, C.-G., & Zang, Y.-F. (2010). DPARSF: A MATLAB toolbox for "pipeline" data analysis of resting-state fMRI. *Frontiers in Systems Neuroscience*, 4, 13.
- Yao, Z., Hu, B., Xie, Y., Zheng, F., Liu, G., Chen, X., & Zheng, W. (2016). Resting-state time-varying analysis reveals aberrant variations of functional connectivity in autism. *Frontiers in Human Neuroscience*, 10, 463.
- Yarkoni, T., Poldrack, R. A., Nichols, T. E., Van Essen, D. C., & Wager, T. D. (2011). Large-scale automated synthesis of human functional neuroimaging data. *Nature Methods*, 8(8), 665–670.
- Yeo, B. T., Krienen, F. M., Sepulcre, J., Sabuncu, M. R., Lashkari, D., Hollinshead, M., Roffman, J. L., Smoller, J. W., Zöllei, L., & Polimeni, J. R. (2011). The organization of the human cerebral cortex estimated by intrinsic functional connectivity. *Journal of Neurophysiology*, 106(3), 1125–1165.
- Yerys, B. E., Gordon, E. M., Abrams, D. N., Satterthwaite, T. D., Weinblatt, R., Jankowski, K. F., Strang, J., Kenworthy, L., Gaillard, W. D., & Vaidya, C. J. (2015). Default mode network segregation and social deficits in autism spectrum disorder: Evidence from non-medicated children. *NeuroImage: Clinical*, 9, 223–232.
- Yu, M., Linn, K. A., Cook, P. A., Phillips, M. L., McClinnis, M., Fava, M., Trivedi, M. H., Weissman, M. M., Shinohara, R. T., & Sheline, Y. I. (2018). Statistical harmonization corrects site effects in functional connectivity measurements from multi-site fMRI data. *Human Brain Mapping*, 39(11), 4213–4227.
- Zabihi, M., Oldehinkel, M., Wolfers, T., Frouin, V., Goyard, D., Loth, E., Charman, T., Tillmann, J., Banaschewski, T., & Dumas, G. (2019). Dissecting the heterogeneous cortical anatomy of autism spectrum disorder using normative models. *Biological Psychiatry: Cognitive Neuroscience and Neuroimaging*, 4(6), 567–578.
- Ziegler, G., Ridgway, G. R., Dahnke, R., Gaser, C., & A. S. D. N. Initiative. (2014). Individualized Gaussian process-based prediction and detection of local and global gray matter abnormalities in elderly subjects. *NeuroImage*, 97, 333–348.

## SUPPORTING INFORMATION

Additional supporting information can be found online in the Supporting Information section at the end of this article.

**How to cite this article:** Li, L., Su, X., Zheng, Q., Xiao, J., Huang, X. Y., Chen, W., Yang, K., Nie, L., Yang, X., Chen, H., Shi, S., & Duan, X. (2022). Cofluctuation analysis reveals aberrant default mode network patterns in adolescents and youths with autism spectrum disorder. *Human Brain Mapping*, 43(15), 4722–4732. <https://doi.org/10.1002/hbm.25986>